Adsorption
https://doi.org/10.1007/s10450-023-00392-0

Adsorption mechanisms of ethane, ethene and ethyne on calcium exchanged LTA and FAU zeolites

Christian Bläker[1] · Volker Mauer[1] · Christoph Pasel[1] · Frieder Dreisbach[2] · Dieter Bathen[1,3]

Received: 13 September 2022 / Revised: 24 May 2023 / Accepted: 29 June 2023

Abstract
The aim of this study is to unravel the influence of single, double and triple bonds in hydrocarbons on the mechanisms of adsorption on zeolites. Therefore, the adsorption of the C2 hydrocarbons ethane, ethene and ethyne on different adsorbents is studied by adsorption calorimetry. As adsorbents pure sodium LTA (NaA) and FAU (NaX) zeolites and calcium exchanged CaNaA and CaNaX zeolites are used. Based on experimental loadings and heat of adsorption, the influence of the number and distribution of cations on different cation positions are discussed in detail. With increasing degree of exchange the increasing number of Ca^{2+}-cations introduce energetically more valuable adsorption sites into the zeolites. On the other hand, the decreasing total number of cations has a negative effect on saturation loading. The impact of these opposing effects and the different occupation of cation positions on the interactions and mechanisms occurring are discussed. The loading increases from ethane to ethene to ethyne and shows higher values on FAU compared to LTA. In terms of interactions, due to the single bond, in ethane only dispersion and induction interactions are formed. In ethene and ethyne due to the double and triple bonds, respectively, additional quadrupole cation and π-interactions occur. In this study, for the first time the formation of a π-complex with Ca^{2+}-cations at position I in LTA and at positions II, III, and III' in FAU is demonstrated. For ethyne, additional π-complex formation with Na^{+}-cations on the identical positions is also detected, which was previously unknown in literature.

Keywords Ethane · Ethene · Ethyne · Faujasite type X zeolite · Heat of adsorption · Linde type A zeolite

1 Introduction

Ethane, ethene and ethyne are important intermediates in chemical industry [1]. Ethene is mostly produced by thermal or catalytic cracking, with ethane and ethyne as minor components. For example, there are typically about 3–5 wt% ethane, 30 wt% ethene and < 1 wt% ethyne in the product of naphtha steam crackers [2]. Separation of ethane and ethene is mainly done by (cryogenic) rectification [3]. Ethyne must either be separated in advance or hydrogenated and thus converted into ethene. Both rectification and hydrogenation are very cost- and energy-intensive processes, with adsorption as an alternative separation process [4]. While separation of binary ethane/ethene mixtures by adsorption, especially on zeolites, is already a subject of research [5–10], the adsorption of ethyne as a pure substance as well as in a mixture has hardly been considered so far. In most studies, the focus is on the determination of equilibrium or kinetics data. However, the mechanisms and interactions occurring during adsorption can only be described and quantitatively determined by additionally measuring the heat of adsorption. Work on the energetic characterization of the adsorption of ethane and ethene on zeolites has already been published in literature.

Dunne et al. investigated the adsorption of ethane on a NaX zeolite by simultaneous measurement of adsorption isotherms and heat of adsorption with a calorimeter. Starting from an initial heat of adsorption of 27.5 kJ/mol, the authors find an increasing heat of adsorption with increasing

✉ Christian Bläker
Christian.blaeker@uni-due.de

[1] Thermal Process Engineering, University of Duisburg-Essen, Lotharstraße 1, 47057 Duisburg, Germany

[2] TA Instruments – a Division of Waters GmbH, Altendorfstraße 10, 32609 Hüllhorst, Germany

[3] Institute of Energy and Environmental Technology e.V. (IUTA), Bliersheimer Straße 60, 47229 Duisburg, Germany

Published online: 11 July 2023

loading. This is explained by dominant adsorbate–adsorbate interactions [11].

Stach et al. investigated adsorption equilibria of ethane and ethene on a NaX zeolite. The authors found higher adsorption capacities of ethene compared to ethane and explain this with additional interactions of the ethene double bond with cations in the zeolite. The additional cation-π interactions lead to a higher heat of adsorption of ethene [12].

Golipour et al. studied the adsorption of ethane and ethene on pure and modified 13X and 5A zeolites. The authors attribute the higher adsorption capacity of ethene compared to ethane, which occurs for all zeolites, to the smaller kinetic diameter and the higher quadrupole moment of ethene. Furthermore, they observe an increase in adsorption capacity with increasing proportion of divalent cations in the zeolites for both ethane and ethene [13].

Carter et al. measured the adsorption of ethene on cation-exchanged faujasite zeolites (AgX, CdX, BaX), by microcalorimetry in the low coverage range up to 0.12. The authors explain the constant heat of adsorption in this loading range by a significantly higher number of cations compared to the number of adsorbed ethene molecules per unit cell. Varying the type of cation changes the heat of adsorption. The authors conclude, that the adsorption of ethene on zeolites is dominated by the ethene-cation interactions rather than the ethene-aluminosilicate interactions [14].

Choudhary et al. investigated the adsorption of ethane and ethene on a NaX zeolite with a Si/Al ratio of 1.3. The isosteric enthalpy of adsorption of ethene calculated by the Clausius-Clapeyron method is about a factor of two larger than the isosteric enthalpy of adsorption of ethane. The higher enthalpy of adsorption of ethene is explained by stronger sorbate-sorbent interactions [15].

Bezus et al. studied the adsorption of ethane and ethene on faujasite type X zeolites modified with different monovalent cations. By measuring isotherms at different temperatures, the isosteric enthalpy of adsorption could be calculated. The authors found that the amount of adsorption and the heat of adsorption of ethene are larger than those of ethane due to specific π-bond interactions of ethene with the zeolite cations. The amount of this contribution decreases with increasing cation radius [16]. In addition, the authors studied the adsorption of ethane and ethene on NaX, CaNaX and SrNaX zeolites at different temperatures. The capacity and heat of adsorption of ethene were larger than for ethane on all zeolites, which the authors attributed to the cation-π interactions between ethene and the cations of the zeolites. The authors also claim that the enthalpy of adsorption depends on the cation charge as well as the number of cations on the accessible sites in the supercage [17].

Triebe et al. investigated the adsorption of ethane and ethene on a 13X, CaX, 4A and 5A zeolite and calculated the enthalpy of adsorption using the van't Hoff method. For both ethane and ethene, the authors found higher enthalpies of adsorption on the zeolites modified with Ca^{2+}-cations (13X and 5A) compared to the pure sodium 13X and 4A zeolites. The authors ascribe the higher enthalpies of adsorption to strong interactions between the divalent Ca^{2+}-cations and the double bond (π-bond) of the ethene molecule [18].

Perez et al. studied the adsorption of ethane and ethene on a commercial 4A zeolite in a temperature range of 293.15–353.15 K using a glass-vacuum volumetric device. To evaluate the interactions, they calculated the isosteric enthalpy of adsorption using the Clausius–Clapeyron equation. They attribute the higher enthalpy of adsorption of ethene compared to ethane in the low loading range to the higher quadrupole moment of ethene. Due to the nonpolar character of ethane, the authors assume that ethane only forms non-specific interactions. They explain the almost constant enthalpy of adsorption of ethane and ethene in the range of low loadings with a compensating effect of the interaction between the adsorbed molecules, which increases with the loading, and the interactions with the surface, which become weaker with the loading due to the heterogeneity of the surface [19].

Studies of ethyne adsorption on zeolites are rare. Harper et al. published equilibrium data of ethane, ethene and ethyne on a 4A zeolite. The highest loading is reported for ethyne, followed by ethene and ethane. The different quadrupole moments are listed as the determining factor for the different loadings. In addition, for ethyne at a loading of 70 cc/g, the authors give the isosteric enthalpy of adsorption as 43 kJ/mol [20]. Further equilibrium data on the adsorption of ethyne can be found on catalysts for acetylene hydrogenation [1, 21, 22].

The literature review shows studies on the energetic description of the adsorption of ethane and ethene on zeolites, but only few data on the adsorption of ethyne. A few measurements on cation-exchanged zeolites can be found, but there is no systematic investigation of the influence of the degree of exchange on the capacity and on the energetic properties. The present work is intended as a first step to fill the data gap. For this purpose, adsorption isotherms and heat of adsorption of ethane, ethene and ethyne are measured. As adsorbents pure sodium LTA (NaA) and FAU (NaX) zeolites and systematically calcium exchanged CaNaA and CaNaX zeolites are used. The focus of the discussion is on the mechanistic elucidation of the interactions of ethane, ethene and ethyne with the zeolites, with particular focus on the influence of the single, double and triple bonds between the C atoms on the adsorption.

2 Experimental

2.1 Adsorbents

Zeolites are primarily composed of aluminum (Al) and silicon (Si) atoms, which are linked via oxygen (O) atoms to SiO_4- and AlO_4-tetrahedra. Following the Löwenstein rule, only Si–O–Si and Si–O–Al links are possible [23]. From SiO_4- and AlO_4-tetrahedra, different secondary building units (SBUs) such as double four rings (D4R) and double six rings (D6R) as well as sodalite cages (β-cage) are formed. By linking eight β-cages via D4R, the LTA zeolite structure is obtained, with the enclosed cavity referred to as an α-cage. In the FAU zeolite structure β-cages are connected via D6R. The cavity enclosed is called super cage [24, 25]. Since AlO_4-tetrahedra introduce a negative charge into the zeolite structure, positively charged cations (mostly alkali or alkaline earth cations) are necessary for neutralization. In Fig. 1 the framework topologies with the theoretical cation positions are illustrated by black dots.

In LTA zeolite, cation site I is located in the α-cage at the surface of six rings (S6R), cation site II is located in the eight-ring (S8R) of the window to the α-cage and cation site III is located in the α-cage at the surface of four-rings (S4R). All cations are freely accessible to adsorptive molecules. Due to the Si/Al ratio of one, 12 charges are required per unit cell of zeolite LTA for charge balance [26, 27].

In FAU zeolite, cation site I is located in the center of a D6R, while cation site I' is located in the β-cage at the interface to a D6R. Cation site II is located in the super cage at the S6R to the β-cage and cation site II' in the β-cage at the S6R to the super cage. Cation site III is the position in the super cage at the S4R to the β-cage and cation site III' is located in the 12-ring window, at the edge of a S4R. Cations on sites I, I', and II' are located in the D6R or the β-cages and are therefore not accessible to C2 hydrocarbons. In contrast, cation sites II, III, and III' are located inside the supercage and therefore can interact with the C2 hydrocarbons. The number of cations in each unit cell of a faujasite zeolite depends on the Si/Al ratio, with a maximum of 96 cations (Si/Al = 1). The distribution of cations to corresponding positions depends on the Si/Al ratio and directly affects the physical and chemical properties of zeolites [28–30]. Since for both LTA and FAU the number of cations actually present is smaller than the number of positions theoretically available, positions may be only partially occupied or not occupied at all.

For adsorption experiments, binder-free Linde Type A and Faujasite Type X zeolite from Chemiewerk Bad Köstritz GmbH (CWK), Bad Köstritz, Germany were used. All zeolites were provided as spherical granules with a particle size of 1.6–2.5 mm. The NaA zeolite has a Si/Al ratio of nearly 1.0 and the NaX zeolite has a Si/Al ratio of 1.175. In addition to these two pure sodium zeolites, further calcium exchanged zeolites, also provided by CWK, were used. Starting from the NaA and NaX zeolite, part of the

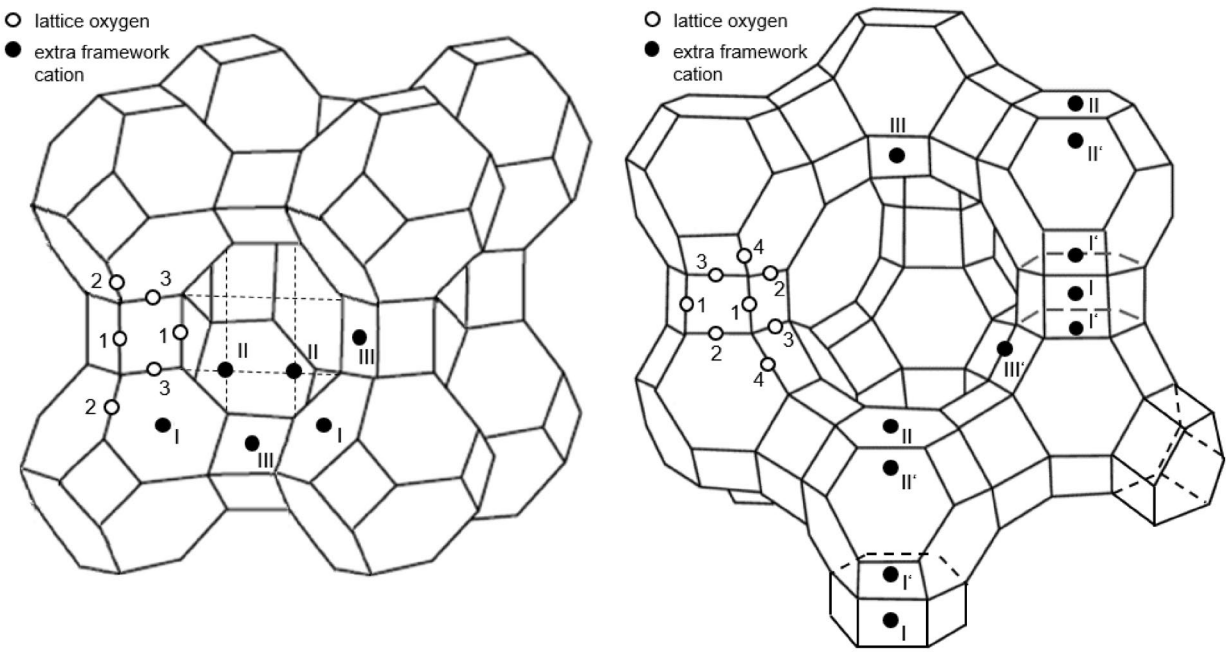

Fig. 1 Structure of Linde Type A (left) and Faujasite Type X (right) zeolite according to [27]

Na^+-cations was exchanged for Ca^{2+}-cations. The exchanged zeolites thus have both Na^+-cations and Ca^{2+}-cations. The ratio of the number of exchanged Na^+-cations to the total number of cations is called the degree of exchange. In the present study, calcium exchanged LTA zeolites with a degree of exchange between 8.7 and 90.0% and calcium exchanged FAU Type X zeolites with a degree of exchange between 22.5 and 87.3% were investigated. Since two monovalent Na^+-cations are exchanged for one divalent Ca^{2+}-cation, the total number of cations decreases with increasing degree of exchange. Table 1 gives an overview of the composition of the zeolites. More information regarding the nomenclature and manufacturing of the zeolites are published in Mauer et al. [26, 31].

The cation distributions in the LTA zeolites, experimentally determined by X-ray powder diffraction (XRPD) [26], is given in the supplementary information (Table S1). The Ca^{2+}-cations first occupy position II and, from a degree of exchange of 46%, also position I. Independent of the degree of exchange, position III is not occupied by Ca^{2+}-cations at all. Since no XRPD measurements are available for the FAU zeolites, the cation distributions for the different degrees of exchange are not precisely known. However, we have already investigated the adsorption of methane on the same FAU zeolites in a previous study [31]. In this study, we were able to determine the cation distributions of the FAU zeolites based on the load-dependent heats of adsorption of methane. The first Ca^{2+}-cations occupy the inaccessible positions I and I'. With increasing degree of exchange above 53%, Ca^{2+}-cations also occupy cation position II, above 67% also positions III, and above 81% also position III'. The obtained cation distributions of the FAU zeolites are consistent with occupation sequences reported in literature and given in the supplementary information (Table S2) [27].

2.2 Adsorptives

As adsorptive, ethane (purity ≥ 99.5%), ethene (purity ≥ 99.9%) and ethyne (purity ≥ 99.9%) from Air Liquide Deutschland GmbH, Germany were used. Ethane C_2H_6 is a member of the homologous series of alkanes. It consists of two sp^3-hybridized carbon atoms (C atoms), each contributing four sp^3-hybrid orbitals. The C atoms are connected by the overlap of two sp^3-hybrid orbitals via a single bond. The electron density of the C–C bond is arranged along the bond axis, resulting in a σ-bond. Each C atom is connected to three hydrogen atoms (H atoms) due to the overlap of the three sp^3-orbitals with the 1 s-orbital of each H atom [3, 32]. The C–H bond is also a σ-bond. The main contaminants in ethane are C_nH_m (n > 2) with 0.2%, methane with 0.1% and ethene with 0.1%. These components may co-adsorb, resulting in higher loadings and thus estimated maximum measurement errors of 5–10%.

Ethene C_2H_4 is the simplest alkene. It consists of two sp^2-hybridized C atoms, each with three sp^2-hybrid orbitals and one 2p-orbital. The two C–H bonds per C atom are

Table 1 Chemical composition of zeolite materials (determined by X-ray fluorescence spectroscopy)

Zeolite	Si/Al ratio	Chemical composition (wt %)				Sodium exchange [%]	Abbreviation
		Al_2O_3	SiO_2	Na_2O	CaO		
Linde type A zeolite							
$Na_{12}Al_{12}Si_{12}O_{48}$	1.0	31.0	35.2	19.6	0.2	0.0	NaA
$Ca_{0.5}Na_{11.0}Al_{12}Si_{12}O_{48}$	1.0	31.8	36.0	18.0	1.5	8.7	CaNaA 8.7
$Ca_{1.1}Na_{9.9}Al_{12}Si_{12}O_{48}$	1.0	31.6	36.0	16.1	3.1	17.6	CaNaA 17.6
$Ca_{1.6}Na_{8.9}Al_{12}Si_{12}O_{48}$	1.0	31.1	35.5	14.2	4.5	26.2	CaNaA 26.2
$Ca_{2.1}Na_{7.7}Al_{12}Si_{12}O_{48}$	1.0	31.3	35.5	12.3	6.1	35.6	CaNaA 35.6
$Ca_{2.8}Na_{6.5}Al_{12}Si_{12}O_{48}$	1.0	30.6	34.9	10.1	7.7	46.0	CaNaA 46.0
$Ca_{4.1}Na_{3.8}Al_{12}Si_{12}O_{48}$	1.0	30.2	34.4	5.7	11.4	68.6	CaNaA 68.6
$Ca_{4.6}Na_{2.8}Al_{12}Si_{12}O_{48}$	1.0	29.9	33.9	4.1	12.6	76.6	CaNaA 76.6
$Ca_{5.0}Na_{2.0}Al_{12}Si_{12}O_{48}$	1.0	30.0	34.0	2.9	13.7	83.0	CaNaA 83.0
$Ca_{5.4}Na_{1.2}Al_{12}Si_{12}O_{48}$	1.0	29.9	34.1	1.5	14.8	90.0	CaNaA 90.0
Faujasite type X zeolite							
$Na_{88}Al_{88}Si_{104}O_{384}$	1.175	28.0	36.9	17.7	0.0	0.0	NaX
$Ca_{10}Na_{68}Al_{88}Si_{104}O_{384}$	1.175	28.3	37.2	13.6	3.5	22.5	CaNaX 22.5
$Ca_{16}Na_{56}Al_{88}Si_{104}O_{384}$	1.175	28.2	37.0	10.9	5.8	37.1	CaNaX 37.1
$Ca_{23}Na_{42}Al_{88}Si_{104}O_{384}$	1.175	28.1	36.7	8.0	8.2	52.9	CaNaX 52.9
$Ca_{29}Na_{30}Al_{88}Si_{104}O_{384}$	1.175	27.6	36.2	5.3	10.2	67.2	CaNaX 67.2
$Ca_{36}Na_{16}Al_{88}Si_{104}O_{384}$	1.175	27.8	36.5	2.9	12.4	81.1	CaNaX 81.1
$Ca_{38}Na_{12}Al_{88}Si_{104}O_{384}$	1.175	28.1	36.9	1.8	13.5	87.3	CaNaX 87.3

formed by overlapping one sp^2-orbital each of the C atom with the 1 s-orbital of each H atom. The C–C σ-bond is formed due to the overlap of the two remaining sp^2-hybrid orbitals of the C atoms. The 2p-orbitals form a C–C π-bond. The electron density is located above and below the molecule plane (see Fig. 2). Due to the simultaneous presence of the C–C σ bond and the C–C π bond, ethene exhibits a C=C double bond [3, 32].

Ethyne C_2H_2 is the simplest alkyne. It consists of two sp-hybridized C atoms, each contributing two sp-hybrid orbitals and two 2p-orbitals. The C–H σ-bond at each C atom is formed as by an overlap of a 1 s-orbital of the H atom with a sp-orbital of the C atom. While a C–C σ bond is formed as a result of overlap of the two remaining sp-orbitals of the C atoms, ethyne additionally has two π bonds between the C atoms formed by two 2p-orbitals being orthogonal to each other at each C atom. The π bonds are so close to each other that they overlap to create a cylindrical π electron cloud, which together with the C–C σ bond forms the C≡C triple bond [3, 32]. In general, electrons in s-orbitals are more strongly attracted to the nucleus than electrons in p-orbitals. Due to the higher proportion of electron density in s orbitals in the sp-hybrid orbitals, the residence probability of the electrons of the C–H bond near the carbon nucleus in alkynes is greater in alkynes than in alkenes (sp^2) and alkanes (sp^3). Thus, the carbon in ethyne is more

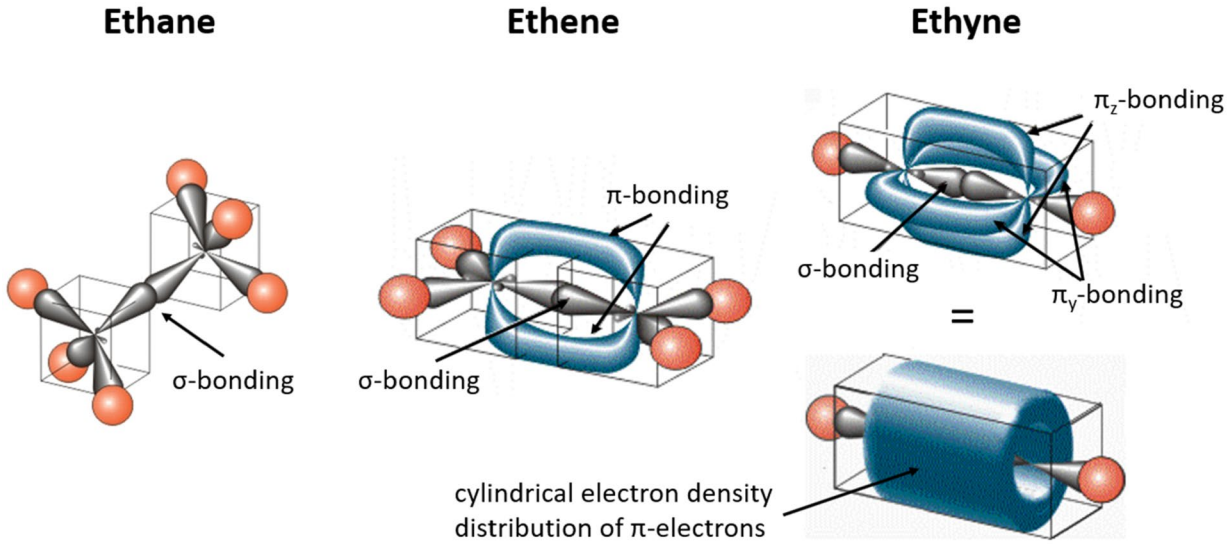

Fig. 2 Structure of ethane, ethene and ethyne

Table 2 Thermodynamic and structural properties of ethane, ethene and ethyne [40–44]

			Ethane	Ethene	Ethyne
Molecular formula			C_2H_6	C_2H_4	C_2H_2
Molar mass	M_A	$[g/mol]$	30.07	28.05	26.04
Molecule dimension (x)	d_{Min1}	$[10^{-10}m]$	3.809	3.280	3.320
Molecule dimension (y)	d_{Min2}	$[10^{-10}m]$	4.079	4.840	5.700
Molecule dimension (z)	d_{Min3}	$[10^{-10}m]$	4.821	4.180	3.340
C–C bond length	l_{C-C}	$[10^{-10}m]$	1.535	1.329	1.203
C–H bond length	l_{C-H}	$[10^{-10}m]$	1.094	1.082	1.060
C–C–H bond angle	ϕ	[°]	111.17	117.20	180.00
Critical temperature	T_{crit}	$[K]$	305.36	282.35	308.40
Acid strength	pK_A	[−]	25	44	50
Saturation vapor pressure (298.15 K)	p_0	$[kPa]$	4180	–	4870
Enthalpy of evaporation (298.15 K)	Δh_V	$[kJ/mol]$	5.16	–	–
Polarizability volume	α	$[10^{-30}m^3]$	4.45	4.25	3.63
Dipole moment	μ	$[10^{-30}Cm]$	0	0	0
Quadrupole moment	θ_{xx}	$[10^{-40}Cm^2]$	2.67	6.67	17.68

electronegative than in ethene and ethane, and ethyne has higher acidity than ethene and ethane (see Table 2) [33].

Ethane is nonpolar and mainly forms induction interactions with cations as well as induction and dispersion interactions with Si–O–Si– or Si–O–Al regions in the zeolite framework. In addition to the mentioned interactions, ethene and ethyne are able to form cation-π interactions with cations due to their π-bonding. Due to the molecular dimensions, steric effects in zeolites can be excluded for all molecules. Table 2 shows the main thermodynamic and structural properties of the adsorptives.

2.3 Experimental apparatus

Before each adsorption experiment, all zeolites are thermally conditioned under vacuum ($< 10^{-7}$ Pa) to desorb water and other molecules. For that purpose, a temperature ramp of 2 K/min is used for heating, which is interrupted by two temperature plateaus at 353.15 K and 393.15 K for 30 min each to avoid a sudden evaporation of adsorbed water. The final temperature of 573.15 K is then maintained for 6 h. The conditioning process is terminated as soon as the pressure rise is less than 3 Pa/min at 573.15 K after 6 h. The residual moisture for zeolite NaA after this conditioning is about 1 wt% and for NaX about 0.4 wt%.

To determine adsorption isotherms and load-dependent heat of adsorption, a commercially available volumetric measuring device (autosorb iQ3, Quantachrome Instruments, Boynton Beach, FL, USA) was coupled with a sensor gas calorimeter developed by Bläker et al. [34, 35]. With the volumetric measuring instrument, pure compound isotherms are measured. Equilibrium is assumed if the change in pressure over a period of 30 min does not exceed a specified threshold. By stepwise increasing the adsorptive concentration, an adsorption isotherm is measured from high vacuum ($< 10^{-7}$ Pa) to ambient pressure (101.3 kPa) at a temperature of 298.15 K. The loading results cumulatively from the sum of the loading differences of all preceding adsorption steps.

The heat released during adsorption is recorded by a sensor gas calorimeter. A detailed description of the experimental setup and procedure as well as the calculations can be found in Bläker et al. [34, 35] and Mauer et al. [31].

3 Results and discussion

In the following, the experimental results are presented as adsorption isotherms and load-dependent heat of adsorption. Adsorption isotherms are shown as loading in molecules per unit cell [MC/UC] as a function of the absolute pressure in kPa. The conversion of the loading from the unit mmol/g to the unit MC/UC is given by Mauer et al. [31]. The load-dependent heat of adsorption is plotted in kJ/mol as a function of the loading in MC/UC. For all measurements, the relative error of the equilibrium loading is about 2.5% and the absolute error of the heat of adsorption is about 1.5 kJ/mol [31, 34, 35]. For reasons of clarity, error bars are not shown in the diagrams. In the isotherm plot, the measured data are plotted as symbols while the isotherms fitted with the Sips equation (Eq. 1) are shown as dashed lines [36].

$$X_{Equ}(T) = X_{mon}(T) * \frac{\left(b_S(T) * p_{A,Equ}\right)^{\frac{1}{n_S(T)}}}{1 + \left(b_S(T) * p_{A,Equ}\right)^{\frac{1}{n_S(T)}}} \quad (1)$$

The Sips parameters monomolecular loading $X_{mon}(T)$, the affinity constant $b_S(T)$ and the heterogeneity constant $n_s(T)$ were determined by fitting to the experimental data using nonlinear regression. All experimental isotherms can be described with very high accuracy ($R^2 > 0.998$). The measured data and the fitted Sips parameters are given in the supplementary information in Tables S3–S20.

3.1 Adsorption on LTA zeolites

Figure 3 (left) shows the adsorption isotherms of ethane on the LTA zeolites with Na^+- and Ca^{2+}-cations. Additionally, in Fig. 3 (right) the isotherms are given using a logarithmic plot of the x-axis to better resolve the range of low pressures. Regardless of the degree of exchange, all isotherms initially rise steeply at low pressure. With increasing pressure, the slope decreases continuously without forming a pronounced plateau. Since the zeolites are binder-free and have no mesopores, the continuously increasing loading indicates a filling of the α-cage and an increase in adsorbate density due to a reorientation of the molecules with increasing pressure. At low pressures the ethane molecules orient themselves energetically optimally towards the cations, which are the primary binding sites. With increasing loading, they presumably orient themselves optimally towards the neighboring molecules as a result of the dominant lateral interactions.

The NaA zeolite, which contains only Na^+-cations, exhibits the lowest loading over the entire pressure range. Up to a degree of exchange of 69%, the loading increases continuously due to the increasing number of energetically more valuable Ca^{2+}-cations and then decreases slightly up to the highest degree of exchange of 90% due to the decreasing total number of cations. As a result, the loading on CaNaA 90.0 at 100 kPa is almost identical to the loading on CaNaA 46.0.

The heat of adsorption of ethane shown in Fig. 4 shows an increase in the initial range from NaA to CaNaA 68.6 and then a decrease to CaNaA 90.0. The order is identical to that determined for methane. The increasing initial heat of adsorption with increasing degree of exchange can be attributed to the cation distribution on energetically different

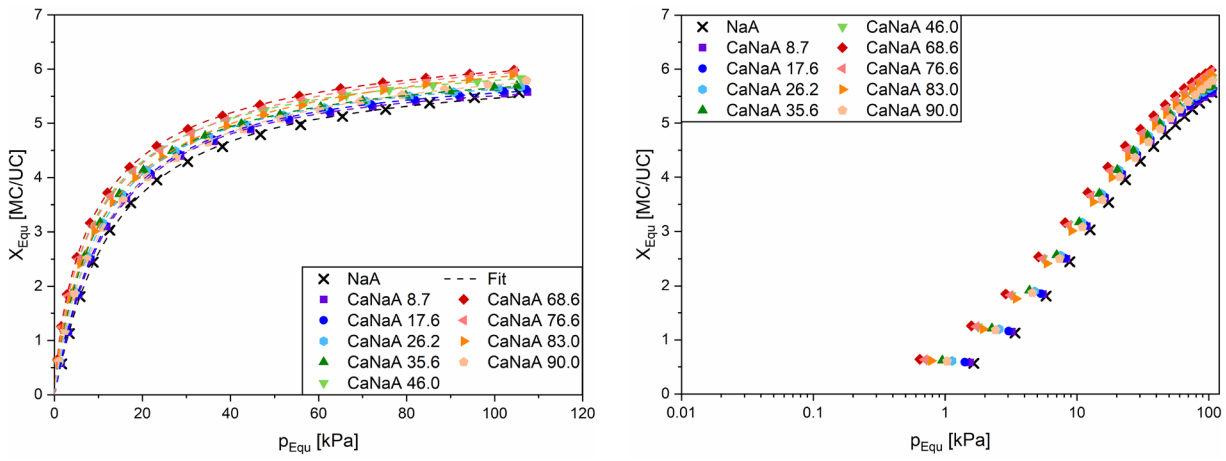

Fig. 3 Adsorption isotherms as linear (left) and logarithmic (right) plot of ethane on NaA and CaNaA zeolites at 25 °C

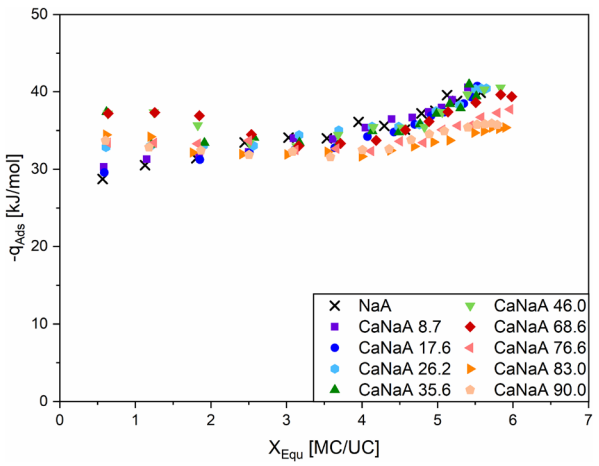

Fig. 4 Heat of adsorption of ethane on NaA and CaNaA zeolites at 25 °C

positions as discussed in detail by Mauer et al. [26]. Stronger and thus energetically more valuable induction interactions occur with the divalent Ca^{2+}-cations compared to the monovalent Na^{+}-cations. While the initial heat of adsorption on NaA is mainly caused by electrostatic interactions of ethane with Na^{+}-cations on I, on CaNaA 8.7 and CaNaA 17.6 additionally interactions with Ca^{2+}-cations on position II and from a degree of exchange of 26% also with Ca^{2+}-cations on I occur [26]. Up to a degree of exchange of 69%, the initial heat of adsorption continues to increase. Since the same cation positions are present and only the number of cations on these positions varies, the increasing heat of adsorption indicates that ethane adsorbs between two cations and can form interactions with both cations. While at a degree of exchange of 69% all cation positions I (4 times Na^{+} and 4 times Ca^{2+}) are occupied, when the degree of exchange is further increased, some of the cation positions I become unoccupied, so that interactions with two cations are only possible to a limited extent and consequently the initial heat of adsorption decreases again.

While pronounced plateaus are formed with increasing loadings for methane, these are not observed for ethane. Only up to a loading of 2 MC/UC a plateau-like heat of adsorption can be identified for zeolites with a degree of exchange above 26% even for ethane. Ethane can presumably form interactions with different combinations of cation positions due to its molecular size. In addition, since the distances to the two cations involved can also vary, a continuous change in the heat of adsorption with increasing loading can be observed instead of pronounced plateaus.

While NaA, CaNaA 8.7 and CaNaA 17.6 show a continuously increasing load-dependent heat of adsorption, all other zeolites first show a decrease of the heat of adsorption (from 0 to 3 MC/UC) and then an increase of the heat of adsorption. The increasing heat of adsorption with increasing loading for NaA, CaNaA 8.7, and CaNaA 17.6 is due to overcompensation of the decreasing interactions with cations by increasing lateral interactions. The overcompensation occurs in these three materials because the strength of the interactions with Na^{+}-cations at site I and Ca^{2+}-cations at site II, as observed in the initial heat of adsorption from the NaA (Na^{+} at I) and the CaNaA 8.7 and CaNaA 17.6 (Ca^{2+} at II), differs only slightly and lateral interactions become stronger as loading increases. However, in the zeolites with a degree of exchange of 26% and above, there are additional Ca^{2+}-cations on cation position I, on which the ethane molecules adsorb first (see Table S1). From a loading of 2 MC/UC, when all adsorption sites on the Ca^{2+}-cations on position I are occupied, with further increasing loading the ethane molecules adsorb on the energetically less valuable Ca^{2+}-cations on position II and Na^{+}-cations on position

I. The difference in energetic contributions is so large that this cannot initially be compensated by the increasing lateral interactions. Consequently, the heat of adsorption initially decreases and an intersection between the heat of adsorption is formed. At this point, comparable adsorption mechanisms are present and presumed interactions with identical adsorption sites are formed. Above a loading of 3 MC/UC the heat of adsorption increases, since the energetic contribution of lateral interactions increases as the number of neighboring molecules increases with loading, resulting in overcompensation.

For loadings above 4 MC/UC, two groups are formed. The zeolites with a degree of exchange greater than 69% show a lower heat of adsorption by about 5 kJ/mol compared to the zeolites with a degree of exchange less than 69%. This is probably due to the fact that with a degree of exchange above 69%, only cation position I is occupied, while II and III remain unoccupied. Since saturation already starts to set in at a pressure of 40 kPa (see Fig. 3 left) and the adsorption sites on position I are already almost completely occupied, with increasing pressure the molecules preferentially adsorb at a larger distance from the cations inside the α-cage as well as in the unoccupied windows between the α-cages. The higher heat of adsorption of zeolites with degrees of exchange lower than 69% is probably due to the cations at position II in the windows between the α-cages. During adsorption inside the α-cage as well as in the windows at the beginning of saturation, induction interactions with the cations on position II can be formed in addition to the lateral interactions, providing an additional energetic contribution.

Adsorption isotherms of ethene on NaA and CaNaA zeolites are shown in Fig. 5 (left). Compared to ethane, the increase at low partial pressure is more pronounced for ethene. When the x-axis is plotted logarithmically (see Fig. 5 (right)), it can be seen that the loading in the initial region increases with increasing degree of exchange. The zeolites with a degree of exchange above 69%, however, show identical loadings. As the pressure continues to increase, the slope in the linear plot decreases continuously. Between 20 and 100 kPa, only the NaA shows a plateau. The CaNaA zeolites, on the other hand, still feature a continuous increase in loading. With increasing degree of exchange up to 69%, the slope of the isotherms increases, so that the isotherm field spreads out. The isotherms with a degree of exchange between 69 and 90% are identical in the pressure range of 20 kPa and 100 kPa and show an identical capacity at 100 kPa of 7.5 MC/UC. The reason for the different patterns at pressures greater than 20 kPa, which can already be seen suggestively in ethane, is probably due to a rearrangement of molecules in the α-cage. The molecules reorient to each other with increasing loading to optimize lateral interactions. At lower loadings, the spatial arrangement of ethene molecules to cations is governed by the optimization of quadrupole-cation interaction. Presumably, this results in ethene molecules being highly angled with respect to each other. From the angled arrangement, the ethene molecules now orient to each other such that the C=C bonds are parallel to each other, while the p-orbitals are orthogonally oriented to each other. This reorientation works particularly well for zeolites where position II is unoccupied or only partially occupied, as this increases the available space for optimized lateral orientation. As a result, as the degree of exchange increases, more reorientation of the molecules and thus higher capacity occur. The effect is more pronounced for ethene than for ethane.

The comparison of the capacities at 100 kPa shows a higher loading of ethene compared to ethane. This is probably due to the higher adsorbate density of ethene. Ethene has four H atoms lying in one plane, while ethane has six

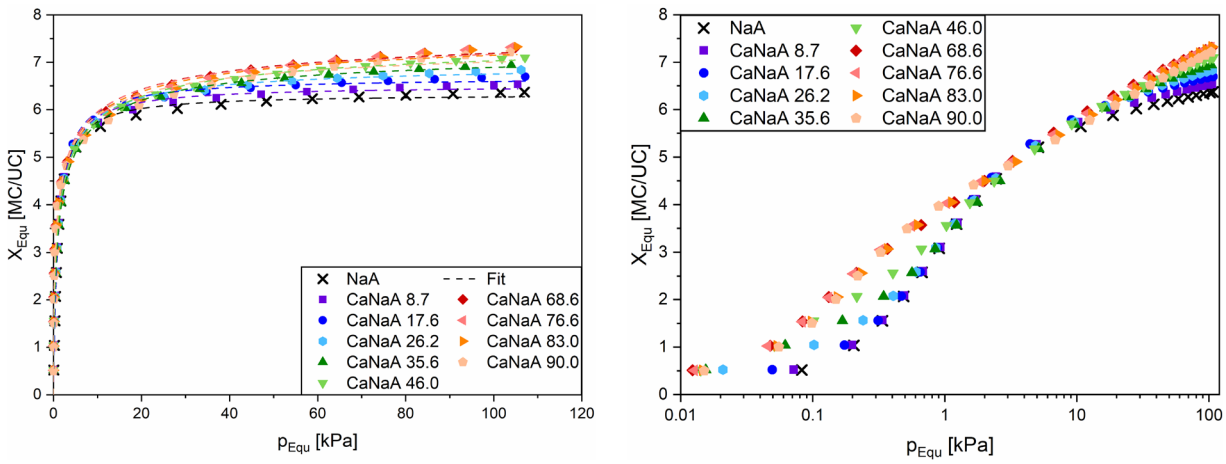

Fig. 5 Adsorption isotherms as linear (left) and logarithmic (right) plot of ethene on NaA and CaNaA zeolites at 25 °C

H atoms projecting at an angle of 111.17° to each other in space.

Figure 6 shows the heat of adsorption of ethene on NaA zeolite and on CaNaA zeolites. Three groups are formed in the initial heat of adsorption depending on the availability of cations on different positions (see Table S1). At 48 kJ/mol, the NaA has the lowest heat of adsorption for ethene. The adsorption is dominated by quadrupole cation interactions with Na^+-cations at the energetically most valuable position I. The second group is formed by CaNaA 8.7 and CaNaA 17.6 with a heat of adsorption of 52 kJ/mol, which is largely due to quadrupole cation interactions with Ca^{2+}-cations at position II. The third group includes the remaining CaNaA zeolites with a degree of exchange ranging from 26 to 90%. The heat of adsorption of about 60 kJ/mol results from interactions with Ca^{2+}-cations at position I which appear in this group due to the high degree of exchange. The zeolites of the third group show an almost identical initial heat of adsorption despite a different number of Ca^{2+}-cations, a different number of cations on the cation positions, and a different total number of cations. This suggests that the first molecules preferentially adsorb directly on a Ca^{2+}-cation at position I and not between two cations as the ethane molecules do. Another indication for this conclusion is that the influence of the cation type is more pronounced in the adsorption of ethene than in the adsorption of ethane. Since the charge number enters quadratically in both induction interactions (as in the case of ethane) and quadrupole cation interactions (as in the case of ethene), the difference cannot be explained by electrostatic interactions. Therefore, it is hypothesized that there is an additional π-complex formation known from complex chemistry in the form of a donor–acceptor interaction [37]. In this case, π-complex formation involves the transfer of electrons from the occupied bonding π molecular orbital of ethene (Lewis base) to the free 4 s-orbital of the Ca^{2+}-cation (Lewis acid) at position I. The π-complex formation occurs in form of a donor–acceptor interaction. Cations at position I are close to the zeolite framework, which presumably allows the negatively charged framework to induce ethene, cause an increase in charge density on one side of the C=C plane, and enhance donor capabilities. Since the plateau length at the heat of adsorption of 60 kJ/mol is only 1–2 MC/UC, only the first 1 to 2 molecules in each unit cell appear to form a π-complex with a cation. The formation of a π-complex requires, first, a Ca^{2+}-cation and, second, a special orientation of the ethene molecule to the corresponding cation. Since the number of available cations at position I is larger than the number of formed π-complexes, apparently the orientation of the molecules is the limiting factor. Presumably, the arrangement is hindered due to the small size of the α-cages and the small distances to the neighboring cations, so that only the first molecules can arrange themselves optimally and form a π-complex. The lower initial heat of adsorption on CaNaA 8.7 and CaNaA 17.6, which have only Ca^{2+}-cations at position II, indicate that this effect does not occur at position II. One reason could be the larger distance between cations on position II and the framework, so that induction with enhanced donor capabilities of ethene is absent. The lower heat of adsorption on NaA also suggests that π-complex formation between the ethene molecules and the Na^+-cation does not occur due to the lower acidity of sodium compared to calcium.

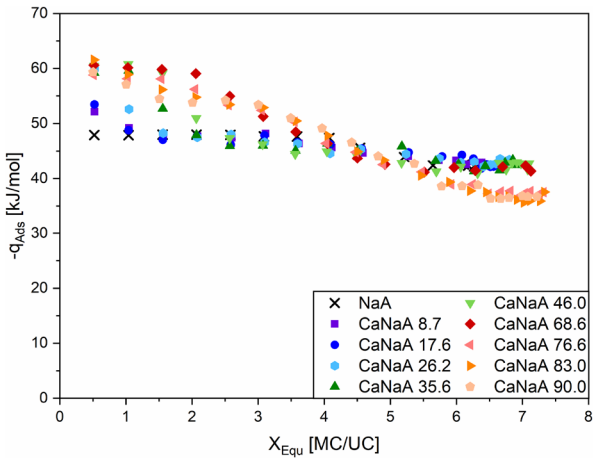

Fig. 6 Heat of adsorption of ethene on NaA and CaNaA zeolites at 25 °C

With increasing loading, all zeolites show a decreasing heat of adsorption for ethene in contrast to ethane. Accordingly, the decreasing energetic contribution of the interactions with the cations and the zeolite framework cannot be compensated by an increase of lateral interactions. This is probably due to two reasons. On the one hand, due to the highly valuable quadrupole cation interactions and the presumed Lewis acid–base interactions, the strength of the interactions with the zeolite decreases more than for ethane as the loading increases. On the other hand, it is possible that due to the supercritical state of ethene, the lateral interactions are weaker than for ethane.

With increasing degree of exchange up to 69%, the heat of adsorption decreases at higher loadings, since the number of energetically valuable sites becomes larger as a result of the increasing number of Ca^{2+}-cations. Since the heat of adsorption decreases again at lower loadings with increasing degree of exchange above 69% despite a higher number of Ca^{2+}-cations, the total number of cations also seems to play a role. Presumably, if no further Lewis acid–base interactions can be formed, ethene adsorbs like ethane between two cations as loading increases and forms interactions with both cations. Thus, the decreasing total number of cations leads to a decrease in heat of adsorption at lower loadings.

For loadings above 5 MC/UC, comparable to ethane, two groups form again with a difference in heat of adsorption of approx. 5 kJ/mol. Here, the difference can probably be explained by occupation of cation position II in zeolites with a degree of exchange of up to 69% and the resulting additional energetic contribution which is missing at a degree of exchange larger than 69%.

Figure 7 on the left shows the adsorption isotherms of ethyne on NaA and CaNaA zeolites. Due to its quadrupole moment, ethyne can form strong interactions with cations, so that a steep slope of the isotherms already occurs at low pressure. When the x-axis is plotted logarithmically (see Fig. 7 (right)), it can be seen that the loading at the first equilibrium point is almost identical for all zeolites up to a pressure of about 0.5 kPa. The isotherms on NaA and on zeolites with a low degree of exchange zeolites are also congruent, but have lower loadings, so a different adsorption mechanism is assumed than for the zeolites with high degree of exchange. With increasing pressure, the slope of all isotherms decreases continuously and becomes approximately linear above a pressure of about 40 kPa. The capacity for ethyne at 100 kPa is almost independent of the degree of exchange. Being 10 MC/UC, the capacity is about 30% higher compared to ethene and ethane. This is due to the lower space requirement, since in linear ethyne all atoms are on one axis and the distance between the two C atoms is shortest at 120 pm due to the triple bond. The effect of spreading, which is observed in ethene, does not occur in ethyne presumably because of the cylindrical π-electron cloud. At low loading, the molecules initially arrange themselves optimally to the cations to maximize interactions. The molecules are presumably angled with respect to each other. As the loading increases, the influence of lateral interactions increases. However, since the π-electron clouds of the molecules reject each other when arranged in parallel, only an orthogonal arrangement in which the positively polarized H-atom of one molecule is oriented toward the negatively polarized π electron cloud of the C≡C triple bond of the neighboring molecule is favorable. Nevertheless, the energetic contribution of this configuration is small. Consequently, no pronounced rearrangement of the molecules with respect to each other probably occurs. The increase in loading, which occurs largely independent of the degree of exchange, indicates that the filling of the α-cages increases uniformly with pressure. The capacity at 100 kPa is approx. 60% larger for ethyne than for ethane and approx. 40% larger than for ethene. Presumably, this is indicative of a decreasing adsorbate density from ethyne to ethene to ethane.

Figure 8 shows the load-dependent heat of adsorption of ethyne on NaA and CaNaA zeolites. The initial heat of adsorption is, like the loading, almost identical for all

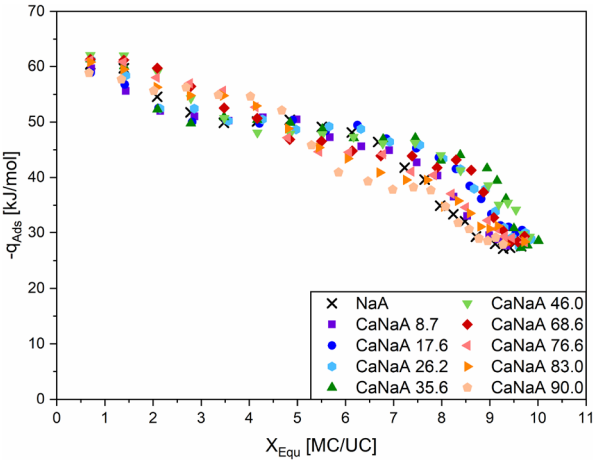

Fig. 8 Heat of adsorption of ethyne on NaA and CaNaA zeolites at 25 °C

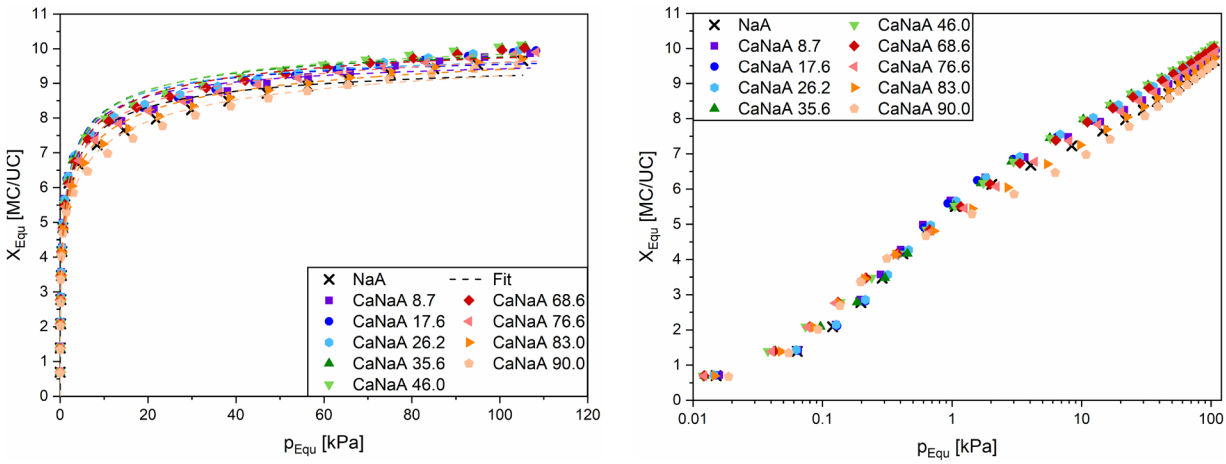

Fig. 7 Adsorption isotherms as linear (left) and logarithmic (right) plot of ethyne on NaA and CaNaA zeolites at 25 °C

zeolites. At 60 kJ/mol, the same value is reached as for the adsorption of ethene on the highly exchanged CaNaA zeolites. On NaA and the low-exchanged CaNaA 8.7 and CaNaA 17.6, however, heat of adsorption are significantly higher by 8–12 kJ/mol compared to adsorption of ethene. In contrast to ethene, ethyne molecules can apparently form π-complexes not only with Ca^{2+}-cations but also with Na^{+}-cations at position I. Here, electrons are transferred from the π-orbitals of the ethyne triple bond to the 3 s-orbital of the Na^{+}-cations. The formation of a π-complex between an Na^{+}-cation and a C≡C triple bond has only been suspected based on solid-state evidence using trimethylsilylacetylene anions (M(C≡C-TMS)2) [38]. Evidence for π- complexation of ethyne with an Na^{+}-cation in zeolites has not been found in literature. Thus, experimental evidence for this mechanism can be provided at this point for the first time. The hypothesis is that ethyne as the stronger donor compared to ethene can donate electrons to both Na^{+}-cations and Ca^{2+}-cations. Ethene, on the other hand, can donate electrons only to Ca^{2+}-cations. However, in the case of bonding between ethyne and Ca^{2+}-cations, a higher bonding enthalpy and thus a higher heat of adsorption would have to be released than in the case of bonding between ethene and Ca^{2+}-cations. However, this is not the case, so that the mechanism is not yet fully understood.

The plateau length of 1–2 MC/UC following the initial heat of adsorption of 60 kJ/mol suggests that only the first 1 to 2 molecules in each unit cell can form a π-complex with a cation. As already observed in the adsorption of ethene, only the first molecules seem to arrange themselves in an optimal way with respect to the cations and form a π-complex due to the small size of the α-cages and the small distances to the neighboring cations. As a consequence, only part of the cations on positions I contributes to π-complex formation.

With increasing loading, the heat of adsorption decreases. The decrease is more pronounced than for ethene due to repulsive lateral interactions resulting from the cylindrical π-electron cloud. In contrast to ethane and ethyne, the heat of adsorptions forms multiple plateaus in ethyne, resulting in a step-like progression. The second plateau-like range with a heat of adsorption of about 50 kJ/mol between 3 and 6 MC/UC occurs presumably due to electrostatic interactions between ethyne and that part of Na^{+}-cations at position I, which cannot form a π-complex. This plateau occurs in the highly exchanged zeolites at slightly lower loadings of 2 to 5 MC/UC and a higher heat of adsorption of 55 kJ/mol as a result of electrostatic interactions with Ca^{2+}-cations at position I. The heat of adsorption in the range between 40 and 45 kJ/mol observed at loadings between 6 and 8 MC/UC are presumably due to interactions (electrostatic or π-complex) with Ca^{2+}-cations (45 kJ/mol) or Na^{+}-cations (40 kJ/mol) at position II. As the degree of exchange increases, a higher number of Ca^{2+}-cations are initially present, resulting in higher heat of adsorption over a larger loading range. On the other hand, from a degree of exchange above 46%, number of Ca^{2+}-cations and Na^{+}-cations on position II decreases, which is why the heat of adsorption also show lower values and continue to decrease even at lower loadings. Finally, at loadings above 8 MC/UC, the heat of adsorption drops to about 30 kJ/mol for all zeolites. The same heat of adsorption indicates that all adsorption sites directly on the cations are already fully occupied, so that with increasing pressure, the molecules adsorb only on the crystal framework or inside the α-cage and form similarly strong interactions.

The energetic value of the different adsorption sites on the Na^{+}-cations and Ca^{2+}-cations at the different cation positions is best discussed in terms of the initial heat of adsorption in Fig. 9. While on the NaA zeolite the heat of adsorption increases from ethane to ethene by about 19 kJ/mol and to ethyne by another 12 kJ/mol, at degrees of exchange above 46% there is a stronger increase from ethane to ethyne at 23 kJ/mol and no further increase to ethyne. It can be seen for the CaNaA zeolites investigated here that with increasing degrees of exchange up to 69%, better adsorption sites are available for ethane and ethene. This is due to the increasing number of Ca^{2+}-cations especially at cation position I. Due to quadrupole-cation interactions and formation of a π-complex with Ca^{2+}-cations at position I, the energetic gain due to cation exchange is more pronounced for ethene compared to ethane. In contrast, almost no effect of the degree of exchange on the initial heat of adsorption is seen for ethyne. This suggests that ethyne can form an energetically similar π-complex with Na^{+}-cations and Ca^{2+}-cations at position I.

3.2 Adsorption on FAU zeolites

The isotherms of ethane on NaX and CaNaX zeolites are shown in Fig. 10. Different shapes of isotherms occur

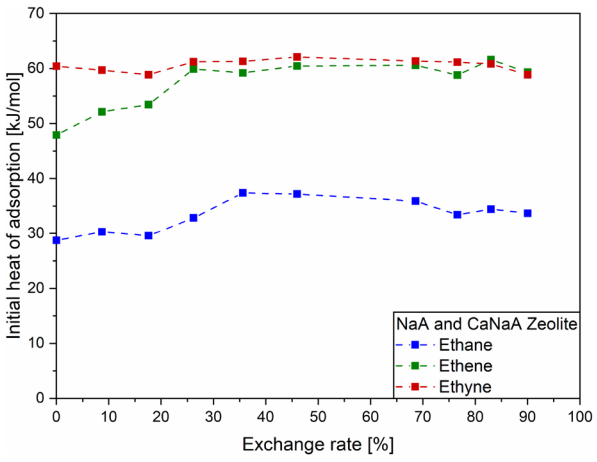

Fig. 9 Initial heat of adsorption as a function of degree of exchange on NaA and CaNaA zeolites at 25 °C

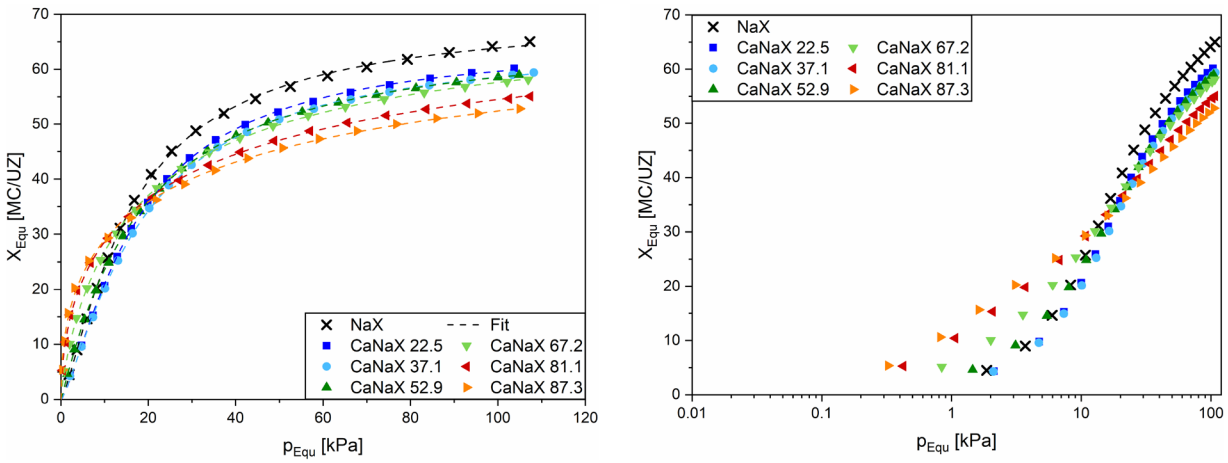

Fig. 10 Adsorption isotherms as linear (left) and logarithmic (right) plot of ethane on NaX and CaNaX zeolites at 25 °C

because, as already discussed in the experimental section, depending on the degree of exchange, different cation positions are occupied differently by Na^+ and Ca^{2+}-cations [31], up to a pressure of 20 kPa, where loading mostly increases with increasing calcium content. The reason for this is that Ca^{2+}-cations, which represent sites of higher energetic value, are already occupied at lower pressure due to the higher adsorption potential. However, the two CaNaX zeolites with the lowest degree of exchange are an exception, as they have a slightly lower loading than the NaX zeolite despite the Ca^{2+}-cations. This is due to the fact that at low calcium exchange, the Ca^{2+}-cations occupy positions I and I', which are localized in the D6R and β-cages, respectively, and are not accessible for adsorption of ethane molecules. Therefore, the ethane molecules can only adsorb on the remaining Na^+-cations, which are present in a smaller number than in NaX.

In the pressure range between 20 and 25 kPa, an intersection of the isotherms occurs, so that the order is reversed. If the pressure increases further, NaX has the highest loading, while with increasing degree of exchange the loading decreases continuously. This is due to the decreasing total number of cations.

Analogous to the initial slope of the isotherms of ethane on NaX and CaNaX zeolites, the initial heat of adsorption in Fig. 11 also mostly increases with the degree of exchange depending on the availability of cations at different positions. Exceptions are again the two CaNaX zeolites with the lowest degrees of exchange, which offer electrostatic interactions only with Na^+-cations. Here, the heat of adsorption is comparable to NaX with 27.5 kJ/mol. A higher initial heat of adsorption of 32 kJ/mol is seen at a degree of exchange of 53%, where Ca^{2+}-cations are also present at position II. The initial heat of adsorption of 35 kJ/mol on CaNaX zeolites with a high degree of exchange can be attributed

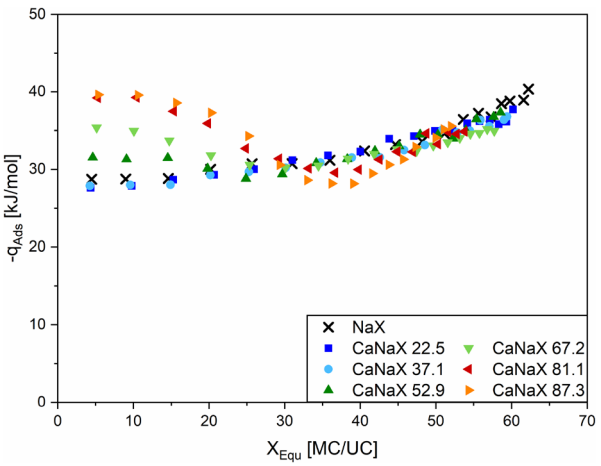

Fig. 11 Heat of adsorption of ethane on NaX and CaNaX zeolites at 25 °C

significantly to interactions with Ca^{2+}-cations at position III and the initial heat of adsorption of 39 kJ/mol to interactions with Ca^{2+}-cations at position III'.

The heat of adsorption of ethane on NaX and on the two low-exchanged zeolites increases continuously with increasing loadings, while the other zeolites initially show a decreasing heat of adsorption and then an increasing heat of adsorption at loadings above about 30 MC/UC. The increasing heat of adsorption with increasing loadings for NaX, CaNaX 22.5, and CaNaX 37.1 is due to overcompensation of the decreasing interactions with Na^+-cations at different cation positions by the increase of lateral interactions. For zeolites with a degree of exchange of 53% and above, the Ca^{2+}-cations also occupy interacting cation positions. Since the difference in energetic values at the various positions is greater for Ca^{2+}-cations than for Na^+-cations, the

decreasing energetic contribution of interactions with cations with increasing loading cannot be compensated by additional lateral interactions. Overcompensation occurs only after all Ca^{2+}-cations are occupied and adsorption occurs on Na^{+}-cations. On CaNaX 52.9 this occurs at about 20 MC/UC and on CaNaX 87.1 at about 40 MC/UC.

Due to the lower total number of cations with increasing degree of exchange, the number of Na^{+}-cations on the interacting positions II, III and III' also decreases. Especially for the highly exchanged CaNaX zeolites, fewer energetically favorable adsorption sites on cations are thus available at loadings above 30 MC/UC, so that the molecules adsorb mainly on the zeolite framework and lower heat of adsorption occur than on NaX.

Figure 12 on the left shows adsorption isotherms of ethene on NaX and CaNaX zeolites. Comparable to the isotherms of ethane, the isotherms of ethene also show different shapes. Due to the different distributions of the Na^{+} and Ca^{2+} cations to the different cation positions depending on the exchange rate, different adsorption mechanisms occur, which result in different loadings. The logarithmic plot (see Fig. 12 (right)) shows that the isotherms on NaX and the two CaNaX zeolites with the lowest degrees of exchange are identical up to a pressure of 1 kPa. From a degree of exchange of 37%, the loading in this pressure range increases continuously with increasing degree of exchange up to 80%, which can be attributed to different adsorption mechanisms. The isotherms of the two highly exchanged zeolites run congruently in the initial range. At a pressure of about 1 kPa, the isotherms intersect. As the pressure continues to increase, the loading increases stronger with increasing exchange rate. By exchanging one divalent Ca^{2+} cation for two monovalent Na^{+} cations, the total number of cations decreases as the exchange rate increases, resulting in the highest loading for the NaX zeolite in the high-pressure zone. Since adsorption of ethene is largely determined by the energetically high valuable quadrupole-cation interactions, the influence of the total number of cations is greater than for the induction and dispersion interactions for ethane, resulting in a more pronounced spreading of the isotherms. The capacity at 100 kPa is about 25% larger compared to ethane. This indicates a higher adsorbate density of ethene.

Heat of adsorption of ethene on NaX and CaNaX zeolites are shown in Fig. 13. The initial heat of adsorption on NaX, CaNaX 22.5 and CaNaX 37.1 are almost identical. Analogous to ethane, interactions occur with Na^{+}-cations at position III'. Due to the additional quadrupole cation interactions, the heat of adsorption is about 43 kJ/mol, about 1.5 times higher than for ethane. As the degree of exchange increases, the initial heat of adsorption increases. As a result of interactions with Ca^{2+}-cations at position II, this is 60 kJ/

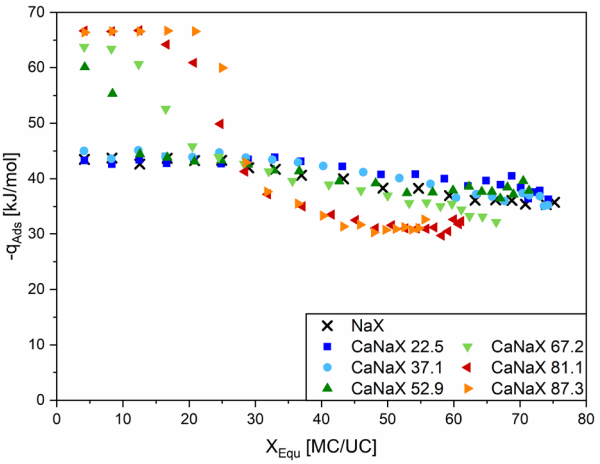

Fig. 13 Heat of adsorption of ethene on NaX and CaNaX zeolites at 25 °C

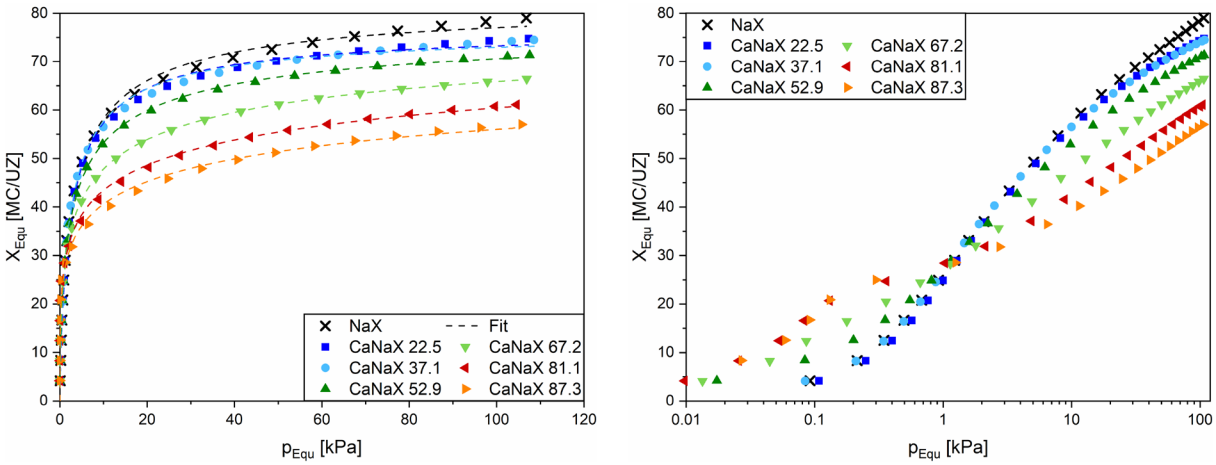

Fig. 12 Adsorption isotherms as linear (left) and logarithmic (right) plot of ethene on NaX and CaNaX zeolites at 25 °C

mol on CaNaX 52.9, 64 kJ/mol with Ca^{2+}-cations at position III on CaNaX 67.2, and 67 kJ/mol with Ca^{2+}-cations at position III' on CaNaX 81.1 and CaNaX 87.3. While the influence of cation position on heat of adsorption is similar to that for ethane, the influence of cation type is more pronounced. Thus, for ethene, the difference in heat of adsorption due to interactions with Na^{+}-cations and with Ca^{2+}-cations at position III' is twice as large at 24 kJ/mol compared to the difference for ethane at only 12 kJ/mol. As in the case of the LTA zeolite, the strong influence of cation type cannot be explained by quadrupole-cation interactions alone. Thus, an additional π-complex formation in form of a donor–acceptor interaction of electrons in the π-orbital of ethene with the 4 s-orbital of Ca^{2+}-cations is also concluded here. Again, the π-complex formation does not seem to be possible for Na^{+}-cations due to the lower acid strength. The different heat of adsorption for interactions with Ca^{2+}-cations at positions II, III, and III' may be due to either different strengths of electrostatic interactions or differently stable π-complexes. Which effect is dominating will be studied in future work. π-complex formation has so far only been detected for the adsorption of ethene on faujasite zeolites with copper, silver and cadmium cations [14, 27, 39]. Here, in addition to electron transfer between the π-orbital of ethene and the 4 s respectively 5 s orbital, a back bonding between the d-orbital of the cations and the π-orbital of ethene occurs. For the adsorption of ethene on exchanged CaX zeolites, the reported data are uncertain, so that so far no clear conclusions about a π-complex formation were possible [14, 39]. A back bonding is excluded due to the lack of a d-orbital.

With increasing loading, heat of adsorption decreases at all zeolites after the energetically most valuable adsorption sites are occupied. Since ethene is supercritical, the energetic contribution of lateral interactions is probably small. Only a small load-dependent decrease is observed for NaX and the two low-exchange CaNaX zeolites. This indicates that the difference in energetic values of Na^{+}-cations is small. Moreover, a sufficient number of cations seems to be present so that all molecules can interact with cations in the studied loading range. As the degree of exchange increases, the load-dependent decrease is more pronounced because the difference in the energetic value of the adsorption sites is larger due to different cation types and cation positions. Especially on CaNaX 81.1 and CaNaX 87.3, it can also be observed that the heat of adsorption for loadings above 26 MC/UC are below those of the other zeolites (see Fig. 13). This indicates that all accessible cations at positions II, III and III' are already occupied and, as the loading increases further, ethene molecules adsorb first on remaining Na^{+}-cations and finally only on the zeolite framework. Due to the assumed negligible energetic contribution of lateral interactions, the constant heat of adsorption of 30 kJ/mol at loadings above 45 MC/UC can be attributed to the energetic contribution of the interactions with the zeolite framework.

The adsorption isotherms of ethyne on NaX and CaNaX zeolites in Fig. 14 (left) feature a steep increase in the range of low loading. Only the logarithmic plot (Fig. 14 (right)) reveals the formation of two groups in the range of low pressures (< 0.5 kPa). The isotherms on NaX, CaNaX 22.5, CaNaX 37.1 and CaNaX 52.9 have an almost identical shape. The isotherms on CaNaX 67.2, CaNaX 81.1 and CaNaX 87.3 have the same shape, but show a higher loading. After passing through an intersection at about 0.5 kPa, NaX exhibits the highest loading. As the degree of exchange increases, loading decreases as in the case of ethene. All isotherms show a slight increase in loading up to the measurement limit of 100 kPa. The capacity at 100 kPa is about 50% larger for ethyne than for ethane and about 30% larger than for ethene, indicating a high adsorbate density of ethyne.

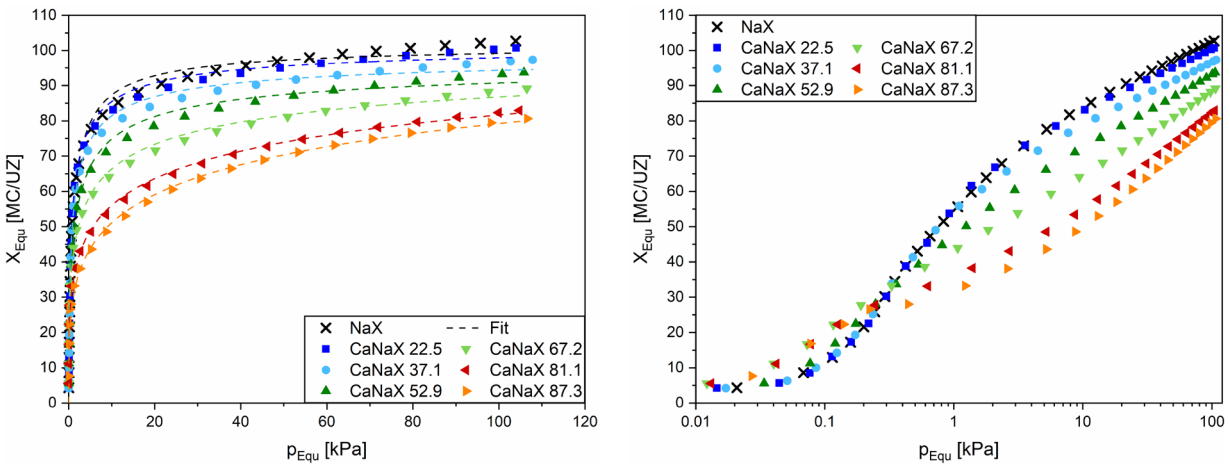

Fig. 14 Adsorption isotherms as linear (left) and logarithmic (right) plot of ethyne on NaX and CaNaX zeolites at 25 °C

The heat of adsorption of ethyne on NaX and CaNaX zeolites are shown in Fig. 15. Up to and including a degree of exchange of 53%, the initial heat of adsorption is about 60 kJ/mol. Accordingly, interactions with Na^+-cations at position III' and with Ca^{2+}-cations at position II have the same energetic value. Since ethyne can form a π-complex with Ca^{2+}-cations, the results provide the first indication that the π-orbitals of the triple bond of ethyne can also form a π-complex with the 3 s orbital of Na^+-cations on FAU zeolites. The higher initial heat of adsorption of 63.5 kJ/mol on CaNaX 67.2 again indicates that the π-complex with a Ca^{2+}-cation at position III is energetically more valuable than with a Ca^{2+}-cation at position II. The energetically most valuable π-complexes are possible with Ca^{2+}-cations at position III' leading to the highest initial heat of adsorption of 66.5 kJ/mol on CaNaX 81.1 and CaNaX 87.3. The initial heat of adsorption of ethene and ethyne on CaNaX 67.2, CaNaX 81.1 and CaNaX 87.3 are identical, respectively. As with the LTA zeolites, this shows that although ethyne is the stronger donor compared to ethene and can donate electron density to both Na^+-cations and Ca^{2+}-cations, the same bonding enthalpy is released. This proves again, that the mechanism is not yet fully understood.

With increasing loading, all zeolites show a decreasing heat of adsorption. This is due to two effects. On the one hand, adsorption takes place with increasing loading at energetically less favorable adsorption sites, as soon as the highest energetic adsorption sites are occupied. On the other hand, repulsive lateral interactions can occur in ethyne as a result of the cylindrical π-electron cloud. Over the entire loading range, heat of adsorption on NaX, CaNaX 22.5 and CaNaX 37.1 is almost congruent. The almost identical load-dependent pattern of the heat of adsorption means that the same adsorption mechanisms occur over the entire loading range. Thus, the number of cations at the accessible cation positions II, III and III' must also be nearly identical. Furthermore, since the initial heat of adsorption is identical, no Ca^{2+}-cations, which are present in different numbers in CaNaX zeolites, are located on these positions. This means that up to a degree of exchange of about 23% Na^+-cations are removed only from positions I, I' or II' and these positions are filled up with Ca^{2+}-cations. According to Yang [27], the occupancy of position I' successively decreases and that of position I increases. Since the strong decrease on CaNaX 37.1 already occurs at a loading of 83 instead of 90 MC/UC on NaX and CaNaX 22.5, this indicates a slightly smaller number of Na^+-cations on the accessible position II, III, III'. Consequently, at a degree of exchange between 23 and 37%, the exchange of Na^+-cations on position II, III or III' now also begins.

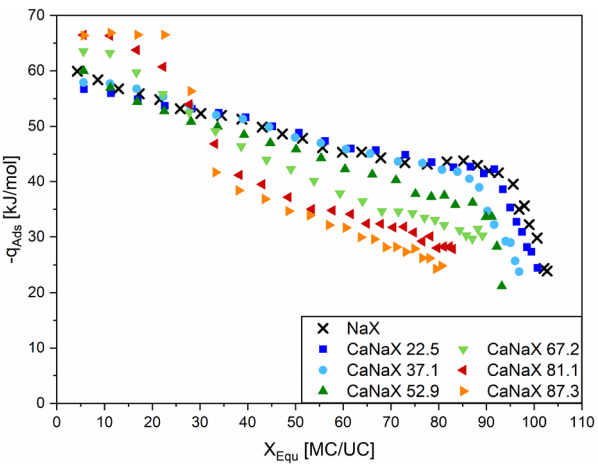

Fig. 15 Heat of adsorption of ethyne on NaX and CaNaX zeolites at 25 °C

As the degree of exchange increases, heat of adsorption drops to lower values even at lower loadings. Since all Ca^{2+}-cations are already saturated, this is due to the lower number of Na^+-cations on the accessible positions II, III and III'. For example, the most exchanged CaNaX 87.3 has 38 Ca^{2+}-cations and only 12 Na^+-cations. As there are 16 Ca^{2+}-cations at position I, there are 22 Ca^{2+}-cations and 12 Na^+-cations at positions II, III and III'. Thus, at a loading of about 38 MC/UC, all adsorption sites on the cations are already occupied by ethyne molecules, so that mainly interactions with the zeolite framework and lateral interactions occur and only a heat of adsorption of about 40 kJ/mol is released. As a result of the constant strength of the interactions with the zeolite framework, the further decrease in heat of adsorption with increasing loading is solely due to repulsive lateral interactions. The difference in heat of adsorption between CaNaX 87.3 and NaX, on the other hand, results from the additional energetic contribution of interactions with Na^+-cations.

While, as shown in Fig. 16, on NaX zeolite the heat of adsorption increases from ethane to ethene by about 15 kJ/mol and to ethyne by another 15 kJ/mol, at a degree of exchange above 80% a stronger increase from ethane to ethene with about 30 kJ/mol and no further increase to ethyne can be seen. For CaNaX zeolites investigated here, it can be seen that up to a degree of exchange of 37%, no influence of cation exchange on the initial heat of adsorption of ethane, ethene and ethyne can be detected, since Ca^{2+}-cations exclusively occupy the inaccessible cation positions I and I'. With further increase in degree of exchange, the initial heat of adsorption increases for all adsorptives as Ca^{2+}-cations first occupy cation position II, followed by III and then III'. While the increase is uniform for ethane, a step is seen between 37 and 53% for ethene. The step is due to the fact that ethene can form a π-complex with Ca^{2+} cations but not with Na^+ cations. Up to an exchange rate of 37%, there are no Ca^{2+} cations on the accessible cation sites II, III

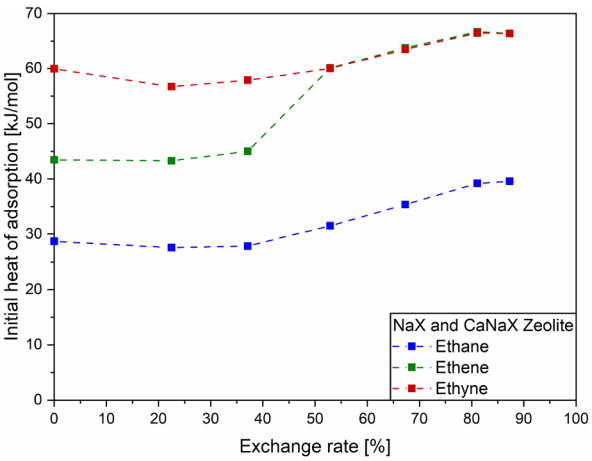

Fig. 16 Initial heat of adsorption as a function of degree of exchange on NaX and CaNaX zeolites at 25 °C

and III'. In contrast, π-complex formation is possible from an exchange rate of 52% since the Ca^{2+} cations occupy also cation site II. This provides an additional energetic contribution and results in a step-like increase of the heat of adsorption. In contrast, since ethyne can also form a π-complex with Na^{+} cations, little influence of the degree of exchange on the initial heat of adsorption is seen for ethyne.

4 Conclusion & outlook

Adsorption of ethane, ethene and ethyne was examined on LTA and FAU zeolites. In addition to zeolites with only sodium cations, calcium-exchanged CaNaA and CaNaX zeolites with systematically varying degrees of exchange were studied.

For the LTA zeolites, an increase in capacity with increasing degree of exchange up to 68% was observed, which can be explained by the increasing number of energetically high valuable adsorption sites on the Ca^{2+}-cations. With a further degree of exchange, the capacity decreases slightly as a result of the decreasing total number of cations. In addition, an increase in capacity from ethane to ethene to ethyne was found mainly due to increasing adsorbate density.

Based on the load-dependent heat of adsorption, with increasing loading, attractive lateral interactions with an additional energetic contribution can be detected for ethane, and repulsive lateral interactions with a negative energetic contribution can be detected for ethyne as a result of the cylindrical π-electron cloud. No significant influence of lateral interactions can be observed for ethene. The initial heat of adsorption increases on NaA with increasing degree of exchange up to 68% and from ethane to ethene and further to ethyne. In contrast, for the CaNaA zeolites, there is a stronger increase from ethane to ethene but no further increase to ethyne. While the increase from ethane to ethene at the zeolite NaA can be attributed to additional quadrupole cation interactions, for the CaNaA zeolites an additional π-complex formation of ethene with Ca^{2+}-cations on position I was detected. Since the initial heat of adsorption of ethyne on all LTA zeolites have almost the same value, a π-complex formation can be detected for ethyne also on Na^{+}-cations at position I, which was previously unknown in the literature. Moreover, the equal heat of adsorption of ethene and ethyne on the CaNaA zeolites with Ca^{2+}-cations at position I indicate energetically equivalent π-complexes. Since ethene and ethyne have a different acidity, differently stable π-complexes would have been expected. However, this is not the case, so the mechanism is not yet fully understood. In order to investigate this effect in more detail, the adsorption of ethane, ethene and ethyne on materials synthesized by a systematic exchange series of LTA with divalent Mg^{2+}, Sr^{2+} und Ba^{2+}-cations will be studied in detail in the future.

On the FAU zeolites, the capacity decreases with increasing degree of exchange, indicating a dominant influence of the decreasing total number of cations versus the increasing number of Ca^{2+} cations. From ethane to ethene and further to ethyne, an increase in capacity is observed, probably as a result of increasing adsorbate density.

The initial heat of adsorption remains constant up to a degree of exchange of 37%, since the exchanged Ca^{2+}-cations exclusively occupy cation positions I, I' and II', which are not accessible for adsorption. With further increasing degree of exchange, the initial heat of adsorption successively increases as cation positions II, III and III' are sequentially occupied by the Ca^{2+}-cations. The initial heat of adsorption for zeolite NaX and for the two low-exchange CaNaX zeolites increases uniformly by 15 kJ/mol from ethane to ethene and further to ethyne. For the zeolites with Ca^{2+}-cations at cation positions II, III and III', the initial heat of adsorption increases more sharply from ethane to ethene and shows identical values for ethene and ethyne. The measured data cannot be explained by electrostatic interactions alone, so a π-complex formation of ethene with Ca^{2+}-cations is suggested. Since the initial heat of adsorption for ethene increases with increasing degree of exchange, either differently stable π-complexes are formed with the Ca^{2+}-cations at positions II, III, and III' or the strength of the additional electrostatic interactions is different. Since the initial heat of adsorption of ethyne on NaX and CaNaX 52.9 are almost identical, π-complex formation can also be found on Na^{+}-cations in FAU zeolites, which was also previously unknown in the literature. The identical heat of adsorption on Ca^{2+}-cations despite the different acidity of ethene and ethyne cannot yet be clearly explained at the FAU either, so that this mechanism is also not yet fully understood. In order to investigate this effect in more detail, in the future

the adsorption of ethane, ethene and ethyne on materials synthesized by a systematic exchange series of FAU with the divalent Mg^{2+}, Sr^{2+} and Ba^{2+} cations will be studied in detail.

Supplementary Information The online version contains supplementary material available at https://doi.org/10.1007/s10450-023-00392-0.

Acknowledgements The Chair of Thermal Process Engineering would like to thank Dr. Jens Zimmermann from Chemiewerk Bad Köstritz GmbH (CWK) for providing the adsorbents.

Author contributions CB Writing—original draft preparation, Writing—review and editing, Formal analysis and investigation, Project administration; VM Writing—original draft preparation, Formal analysis and investigation, Prepared the figures; CP Project administration; FD Development or design of methodology; DB Funding acquisition, Supervision; All authors read and approved the final manuscript.

Funding Open Access funding enabled and organized by Projekt DEAL. We acknowledge support by the Open Access Publication Fund of the University of Duisburg-Essen. This project was supported by the German Research Foundation within the DFG project BA 2012/12-1.

Data availability The online version contains additional material where the cation distributions of the LTA and FAU zeolites, the fitted isotherm parameters, and the measured data of the adsorption isotherms and heats of adsorption can be accessed.

Declarations

Competing interests The authors declare that they have no known competing financial interests or personal relationships that could have appeared to influence the work reported in this paper.

Ethical approval Not applicable.

References

1. Huang, W., Mccormick, J., Lobo, R., Chen, J.: Selective hydrogenation of acetylene in the presence of ethylene on zeolite-supported bimetallic catalysts. J. Catal. **246**(1), 40–51 (2007). https://doi.org/10.1016/j.jcat.2006.11.013
2. Matar, S., Hatch, L.F.: Chemistry of Petrochemical Processes: Provides Quick and Easy Access to Hundreds of Reactions, Processes, and Products, 2nd edn. Gulf Professional Publ, Boston (2001)
3. Speight, J.G.: Handbook of Industrial Hydrocarbon Processes. Gulf Professional, Oxford (2009)
4. Eldridge, R.B.: Olefin/paraffin separation technology: a review Ind. Eng. Chem. Res. **32**(10), 2208–2212 (1993). https://doi.org/10.1021/ie00022a002
5. Aguado, S., Bergeret, G., Daniel, C., Farrusseng, D.: Absolute molecular sieve separation of ethylene/ethane mixtures with silver zeolite A. J. Am. Chem. Soc. **134**(36), 14635–14637 (2012). https://doi.org/10.1021/ja305663k
6. Berlier, K., Olivier, M.-G., Jadot, R.: Adsorption of methane, ethane, and ethylene on zeolite. J. Chem. Eng. Data **40**(6), 1206–1208 (1995). https://doi.org/10.1021/je00022a011
7. Hosseinpour, S., Fatemi, S., Mortazavi, Y., Gholamhoseini, M., Ravanchi, M.T.: Performance of CaX zeolite for separation of C 2 H 6, C 2 H 4, and CH 4 by adsorption process capacity, selectivity, and dynamic adsorption measurements. Sep. Sci. Technol. **46**(2), 349–355 (2010). https://doi.org/10.1080/01496395.2010.508478
8. Hyun, S.H., Danner, R.P.: Equilibrium adsorption of ethane, ethylene, isobutane, carbon dioxide, and their binary mixtures on 13X molecular sieves. J. Chem. Eng. Data **27**(2), 196–200 (1982). https://doi.org/10.1021/je00028a029
9. Mofarahi, M., Salehi, S.M.: Pure and binary adsorption isotherms of ethylene and ethane on zeolite 5A. Adsorption **19**(1), 101–110 (2013). https://doi.org/10.1007/s10450-012-9423-1
10. Narin, G., Martins, V.F., Campo, M., Ribeiro, A.M., Ferreira, A., Santos, J.C., Schumann, K., Rodrigues, A.E.: Light olefins/paraffins separation with 13X zeolite binderless beads. Sep. Purif. Technol. **133**, 452–475 (2014). https://doi.org/10.1016/j.seppur.2014.06.060
11. Dunne, J.A., Rao, M., Sircar, S., Gorte, R.J., Myers, A.L.: Calorimetric heats of adsorption and adsorption isotherms2. O 2 , N 2 , Ar, CO 2 , CH 4 , C 2 H 6 , and SF 6 on NaX, H-ZSM-5, and Na-ZSM-5 zeolites. Langmuir **12**(24), 5896–5904 (1996). https://doi.org/10.1021/la960496r
12. Stach, H., Lohse, U., Thamm, H., Schirmer, W.: Adsorption equilibria of hydrocarbons on highly dealuminated zeolites. Zeolites **6**(2), 74–90 (1986). https://doi.org/10.1016/S0144-2449(86)80001-X
13. Golipour, H., Mokhtarani, B., Mafi, M., Moradi, A., Godini, H.R.: Experimental measurement for adsorption of ethylene and ethane gases on copper-exchanged zeolites 13X and 5A. J. Chem. Eng. Data **65**(8), 3920–3932 (2020). https://doi.org/10.1021/acs.jced.0c00251
14. Carter, J.L., Yates, D.J.C., Lucchesi, P.J., Elliott, J.J., Kevorkian, V.: The adsorption of ethylene on a series of near-faujasite zeolites studied by infrared spectroscopy and calorimetry. J. Phys. Chem. **70**(4), 1126–1136 (1966). https://doi.org/10.1021/j100876a026
15. Choudhary, V.R., Mayadevi, S.: Adsorption of methane, ethane, ethylene, and carbon dioxide on X, Y, L, and M zeolites using a gas chromatography pulse technique. Sep. Sci. Technol. **28**(8), 1595–1607 (1993). https://doi.org/10.1080/01496399308018060
16. Bezus, A.G., Kiselev, A.V., Sedlaček, Z., Du, P.Q.: Adsorption of ethane and ethylene on X-zeolites containing Li +, Na +, K +, Rb + and Cs + cations. Trans. Faraday Soc. **67**, 468–482 (1971). https://doi.org/10.1039/TF9716700468
17. Bezus, A., Kiselev, A., Du, P.Q.: The influence of size, charge and concentration of exchange cations on the adsorption of ethane and ethylene by zeolites. J. Colloid Interface Sci. **40**(2), 223–232 (1972). https://doi.org/10.1016/0021-9797(72)90012-4
18. Triebe, R.W., Tezel, F.H., Khulbe, K.C.: Adsorption of methane, ethane and ethylene on molecular sieve zeolites. Gas Sep. Purif. **10**(1), 81–84 (1996). https://doi.org/10.1016/0950-4214(95)00016-X
19. Romero-Pérez, A., Aguilar-Armenta, G.: Adsorption kinetics and equilibria of carbon dioxide, ethylene, and ethane on 4A(CECA) zeolite. J. Chem. Eng. Data **55**(9), 3625–3630 (2010). https://doi.org/10.1021/je100215c

20. Harper, R.J., Stifel, G.R., Anderson, R.B.: Adsorption of gases on 4A synthetic zeolite Can. J. Chem. **47**(24), 4661–4670 (1969). https://doi.org/10.1139/v69-770
21. Lee, C.J., Sharp, M.A., Smith, R.S., Kay, B.D., Dohnálek, Z.: Adsorption of ethane, ethene, and ethyne on reconstructed Fe3O4(001). Surf. Sci. **714**, 121932 (2021). https://doi.org/10.1016/j.susc.2021.121932
22. Sassen, N.R.M., den Hartog, A.J., Jongerius, F., Aarts, J.F.M., Ponec, V.: Adsorption and reactions of ethyne. Effects of modifiers and formation of bimetallics. Faraday Discuss Chem. Soc. **87**, 311 (1989). https://doi.org/10.1039/DC9898700311
23. Löwenstein, W.: The distribution of aluminum in the tetrahedra of silicates and aluminates. Am. Miner. **39**, 92–96 (1954)
24. Kulprathipanja, S. (ed.): Zeolites in Industrial Separation and Catalysis. Wiley, Weinheim (2010)
25. Xu, R.: Chemistry of Zeolites and Related Porous Materials: Synthesis and Structure. Wiley, Chichester (2007)
26. Mauer, V., Petersen, H., Bläker, C., Pasel, C., Weidenthaler, C., Bathen, D.: Combination of X-ray powder diffraction and adsorption calorimetry for the characterization of calcium exchanged LTA zeolites. Microporous Mesoporous Mater. **337**, 111940 (2022). https://doi.org/10.1016/j.micromeso.2022.111940
27. Yang, R.T.: Adsorbents: Fundamentals and Applications. Wiley, Hoboken (2003)
28. Olson, D.H.: The crystal structure of dehydrated NaX. Zeolites **15**(5), 439–443 (1995). https://doi.org/10.1016/0144-2449(95)00029-6
29. Vitale, G., Mellot, C.F., Bull, L.M., Cheetham, A.K.: Neutron diffraction and computational study of zeolite NaX: influence of SIII' cations on its complex with benzene. J. Phys. Chem. B **101**(23), 4559–4564 (1997). https://doi.org/10.1021/jp970393x
30. Zhu, L., Seff, K.: Reinvestigation of the crystal structure of dehydrated sodium zeolite X. J. Phys. Chem. B **103**(44), 9512–9518 (1999). https://doi.org/10.1021/jp9918171
31. Mauer, V., Bläker, C., Pasel, C., Bathen, D.: Energetic characterization of faujasite zeolites using a sensor gas calorimeter. Catalysts **11**(1), 98 (2021). https://doi.org/10.3390/catal11010098
32. Atkins, P.W.: Physikalische Chemie, 5th edn. Wiley, Weinheim (2013)
33. Smith, M.B., March, J.: March's Advanced Organic Chemistry: Reactions, Mechanisms, and Structure, 6th edn. Wiley, New York (2007)
34. Bläker, C., Pasel, C., Luckas, M., Dreisbach, F., Bathen, D.: Investigation of load-dependent heat of adsorption of alkanes and alkenes on zeolites and activated carbon. Microporous Mesoporous Mater. **241**, 1–10 (2017). https://doi.org/10.1016/j.micromeso.2016.12.037
35. Bläker, C., Pasel, C., Luckas, M., Dreisbach, F., Bathen, D.: A study on the load-dependent enthalpy of adsorption and interactions in adsorption of C5 and C6 hydrocarbons on zeolites 13X and ZSM-5 and an activated carbon. Microporous Mesoporous Mater. **302**, 110205 (2020). https://doi.org/10.1016/j.micromeso.2020.110205
36. Do, D.D.: Adsorption Analysis: Equilibria and Kinetics Series on Chemical Engineering, vol. 2. Imperial College Press, London (1998)
37. Thum, K., Martin, J., Elsen, H., Eyselein, J., Stiegler, L., Langer, J., Harder, S.: Lewis acidic cationic strontium and barium complexes. Eur. J. Inorg. Chem. **2021**(26), 2643–2653 (2021). https://doi.org/10.1002/ejic.202100345
38. Hu, J., Barbour, L.J., Gokel, G.W.: Solid-state evidence for pi-complexation of sodium and potassium cations by carbon-carbon triple bonds. J. Am. Chem. Soc. **123**(38), 9486–9487 (2001). https://doi.org/10.1021/ja0112137
39. Habgood, H.W.: Adsorptive and gas chromatographic properties of various cationic forms of zeolite X. Can. J. Chem. **42**(10), 2340–2350 (1964). https://doi.org/10.1139/v64-342
40. Buckingham, A.D., Disch, R.L., Dunmur, D.A.: Quadrupole moments of some simple molecules. J. Am. Chem. Soc. **90**(12), 3104–3107 (1968). https://doi.org/10.1021/ja01014a023
41. Haynes, W.M. (ed.): CRC Handbook of Chemistry and Physics: A Ready-Reference Book of Chemical and Physical Data, 97th edn. CRC Press, Boca Raton (2017)
42. Pritchard, R.H., Kern, C.W.: Bond moments in the two-carbon series ethane, ethylene, and acetylene. J. Am. Chem. Soc. **91**(7), 1631–1635 (1969). https://doi.org/10.1021/ja01035a008
43. Reid, C.R., Thomas, K.M.: Adsorption kinetics and size exclusion properties of probe molecules for the selective porosity in a carbon molecular sieve used for air separation. J. Phys. Chem. B **105**(43), 10619–10629 (2001). https://doi.org/10.1021/jp0108263
44. Webster, C.E., Drago, R.S., Zerner, M.C.: Molecular dimensions for adsorptives. J. Am. Chem. Soc. **120**(22), 5509–5516 (1998). https://doi.org/10.1021/ja973906m